Cyclic Voltammetric and Scanning Electrochemical Microscopic Study of Menadione Permeability through a Self-Assembled Monolayer on a Gold Electrode

ARTICLE *in* LANGMUIR · AUGUST 2002

Impact Factor: 4.46 · DOI: 10.1021/la0258906

3 AUTHORS, INCLUDING:

Frederic Kanoufi
Paris Diderot University
119 PUBLICATIONS **1,716** CITATIONS

Cyclic Voltammetric and Scanning Electrochemical Microscopic Study of Menadione Permeability through a Self-Assembled Monolayer on a Gold Electrode

Céline Cannes,[†] Frédéric Kanoufi,[‡] and Allen J. Bard*,[†]

Department of Chemistry and Biochemistry, The University of Texas at Austin, Austin, Texas 78312, and Laboratoire Environnement et Chimie Analytique, ESPCI, 10 rue Vauquelin, 75231 Paris Cedex 05, France

Received May 1, 2002. In Final Form: May 8, 2002

Menadione (2-methyl-1,4-naphthoquinone) reduction and menadiol oxidation at octadecanethiol ($C_{18}SH$) monolayer modified gold electrodes were investigated by cyclic voltammetry (CV) and scanning electrochemical microscopy (SECM). The modified electrode acts as a better barrier toward the ferrocyanide transport than toward the menadione species. This difference is attributed to permeation of the organic substrates into the hydrophobic monolayer. A simple model is proposed and applied to extract the rate constant of the kinetically limiting permeation step from the cyclic voltammograms. However, a better estimate of the transport properties is obtained by SECM. The same trends are observed with CV and SECM, and a similar pH dependence shows the loss of an intermediate formed during menadione reduction from the monolayer with increasing pH. This loss can probably be assigned to the rapid expulsion of the more hydrophilic reduced species from the monolayer.

Introduction

Vitamins of the K-group are quinones involved in many biological and physiological systems. The K-vitamin properties can be attributed to their ability to transport both electrons and protons. Thus, these compounds are mainly used as antihemorrhagic agents,[1] but they are also involved in photosynthetic mechanisms,[2] cellular respiration,[3] and oxidative phosphorylation.[4] For these reasons, knowledge of the redox and the transport properties of quinones is important for a better understanding of their behavior in biological environments. Quinone reduction at metallic electrodes in organic solvents in the presence and absence of protons or in aqueous solutions is well documented[5] and involves a global transfer of two electrons and two protons to provide the associated hydroquinone. In the special case of menadione (2-methyl-1,4-naphthoquinone), a K-vitamin (menadione is also known as vitamin K3), this process is described by eq 1.[6−8]

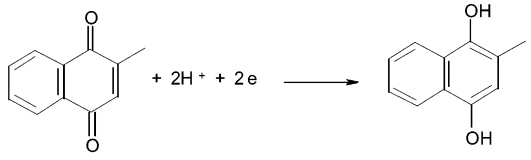

menadione menadiol (1)

Several authors have also investigated the electrochemical properties of vitamin K and other quinones in biomimetic membrane systems. For such purposes, quinones could be immobilized on electrodes either by adsorption[9,10] or by incorporation into a self-assembled monolayer.[11−14] Even when the quinone is immobilized in a lipophilic environment, electron and proton transfers are able to occur.

Scanning electrochemical microscopy (SECM) is a useful technique for the localized sensing of electron, ion, and molecular transport in a wide range of materials.[15,16] It has been used for the investigation of transport in biomimetic systems, such as solid/liquid interfaces modified with self-assembled mono-[17−20] and bilayers,[18] liquid/liquid interfaces modified with mono-[21] and bilayers,[22−24] or air/water interfaces modified with a monolayer.[25]

We have previously reported on SECM studies of the electrochemical oxidation of ferrocenemethanol and ferrocyanide at mono- and bilayer modified electrodes.[18] In that study we showed that oxidation only occurred at defects (pinholes) in the layers. In light of work on incorporated quinone in monolayer covered electrodes[11−13]

[†] The University of Texas at Austin.

[‡] ESPCI.

(1) Bjornsson, T. D. In *Effects of Drugs on Nutrition*; Roe, D. A., Campbell, T. C., Eds.; Marcel Dekker: New York, 1982; p 114.
(2) Pennock, J. F. In *Vitamin A, E, und K*; Von Kress, H. F., Blum, K. U., Schattauer, F. K., Eds.; Verlag: Stuttgart, 1969; p 181.
(3) Brodie, A. F.; Watanabe, T. *Vitam. Horm. (Leipzig)* **1966**, *24*, 447.
(4) Lederer, E.; Vilkas, M. *Vitam. Horm. (Leipzig)* **1966**, *24*, 409.
(5) Chambers, J. Q. In *The Chemistry of the Quinonoid Compounds*; Patai, S., Ed.; John Wiley: New York, 1974; pp 737−791.
(6) Ksenzhek, O. S.; Petrova, S. A.; Kolodyazhny, M. V.; Oleinik, S. V. *Bioelectrochem. Bioenerg.* **1977**, *4*, 335.
(7) Vallot, R.; N'Diaye, A.; Bermont A.; Jakubowicz, C.; Yu, L. T. *Electrochim. Acta* **1979**, *25*, 1501.
(8) Zhu, Z.; Li, N.-Q. *Electroanalysis* **1999**, *15*, 1145.
(9) Gordillo, G. J.; Schiffrin, D. J. *J. Chem. Soc., Faraday Trans.* **1994**, *90*, 1913.
(10) Kats, E. Y.; Solov'ev, A. A. *J. Electroanal. Chem.* **1990**, *291*, 171.
(11) Takehara, K.; Takemura, H.; Ide, Y. *J. Electroanal. Chem.* **1991**, *308*, 345.
(12) Marchal, D.; Boireau, W.; Laval, J. M.; Bourdillon, C.; Moiroux, J. *J. Electroanal. Chem.* **1998**, *451*, 139.
(13) Herrero, R.; Tadini Buoninsegni, F.; Becucci, L.; Moncelli, M. R. *J. Electroanal. Chem.* **1998**, *445*, 71.
(14) Moncelli, M. R.; Becucci, L.; Nelson, A.; Guidelli, R. *Biophys. J.* **1996**, *70*, 2716.
(15) Bard, A. J.; Fan, F.-R. F.; Mirkin, M. V. In *Electroanalytical Chemistry*; Bard, A. J., Ed.; Marcel Dekker: New York, 1994; Vol. 18, p 243.
(16) Bard, A. J., Mirkin, M. V., Eds. *Scanning Electrochemical Microscopy*; Marcel Dekker: New York, 2001.
(17) Forouzan, F.; Bard, A. J.; Mirkin, M. V. *Isr. J. Chem.* **1997**, *37*, 155.
(18) Cannes, C.; Kanoufi, F.; Bard, A. J. *Langmuir*, submitted.
(19) Wittstock, G.; Hesse, R.; Schuhmann, W. *Electroanalysis* **1997**, *9*, 746.
(20) Wittstock, G.; Schuhmann, W. *Anal. Chem.* **1997**, *69*, 5059.

10.1021/la0258906 CCC: $22.00
Published on Web 08/31/2002

and since *p*-hydroquinone permeation through protoplast cell membranes could be detected with a microelectrode,[26] we would expect that the hydrophobic and lipid soluble[27] menadione species would permeate an organic monolayer assembled on a gold electrode. We report here the use of SECM to study the permeation process for a monolayer immobilized at gold electrode. The monolayer was prepared by adsorption of octadecanethiol ($C_{18}SH$) on a gold electrode surface. Such hydrophobic monolayers adsorbed on gold surfaces are electronically insulating against hydrophilic compounds such as ferrocene derivatives[17,18,28] and inorganic complexes.[29]

Experimental Section

Chemical Reagent. Octadecanethiol (Aldrich), 2-methyl-1,4-naphthoquinone (Aldrich), sodium ferrocyanide (Aldrich), and sodium chloride (EM) were used without further purification. Ethanol was absolute analytical grade. All solutions are prepared with deionized water (Milli-Q, Millipore Corp.).

Electrosynthesis of Menadiol. The menadiol was synthesized by bulk electrolysis at −0.3 V under nitrogen atmosphere to avoid its easy oxidation. The cathode was a mercury pool, the anode, a silver wire, and the reference electrode, Ag/AgCl. The cathode compartment was filled with a menadione solution in phosphate buffer, and the anode compartment, with aqueous 0.1 M NaCl. The electrolysis was monitored by CV at a carbon (7 μm diameter) SECM tip and was stopped when all of the menadione had been reduced.

Preparation of the Monolayer. The gold electrode was a gold wire (0.07 cm^2) inserted in Teflon. This electrode was first polished carefully with 0.3 and 0.05 μm alumina and then sonicated in water for 15 min followed by EtOH for 2−3 min. After the electrode was cleaned with hot sulfuric acid and rinsed with water, several scans were taken in the range −0.3 to 1.5 V (vs Ag/AgCl) in freshly prepared deoxygenated 0.5 M H_2SO_4. The electrode was then rinsed with water and EtOH, dried in air, and immersed finally in an absolute EtOH solution of 5 mM octadecanethiol overnight. Before electrochemical measurements, the electrode was rinsed with EtOH and dried in a stream of pure nitrogen or argon.

Measurements. Electrochemical experiments were carried out with a CHI-900 electrochemical workstation (CH Instruments, Austin, TX), employing a three-electrode cell: the gold electrode acted as the working electrode, a platinum wire as the counter electrode, and a Ag/AgCl wire as the reference electrode. All potentials are reported with respect to this reference. The approach curves were made with a carbon (7 μm diameter) SECM tip. They were reproduced at least at two different locations on the filmed substrate.

Digital Simulations of the voltammograms were performed with the software package DigiSim (Bioanalytical Systems, version 2.1).

Results and Discussion

Comparison of the Electrochemical Behavior of Menadione and Ferrocyanide. To compare the electrochemical behavior of menadione with that of a compound that cannot permeate the monolayer, $Fe(CN)_6^{4-}$, CV was carried out at the Au electrode and at the same $C_{18}SH$/Au electrode as that used for the menadione experiments (Figure 1). $Fe(CN)_6^{4-}$ is oxidized in a one-electron reaction ($E°$ = 0.226 V; α = 0.4; $k°$ = 0.03 cm s^{-1}).[30] In the presence of the monolayer, the current decreased considerably and became mainly capacitive. The long alkane chains of the adsorbed thiol on gold are densely packed and well organized and act as an effective electron and ion barrier.[31] Thus, in the presence of the monolayer, $Fe(CN)_6^{4-}$ cannot approach the electrode surface and its apparent heterogeneous electron transfer rate clearly decreases. The electron transfer at such an electrode is described[32] to occur in one of three ways: (1) by a tunneling process; (2) by permeation of the redox species into the film and electron transfer; and (3) by diffusion of the electroactive compound inside pinhole or defect sites and electron transfer only at the exposed electrode surface. As previously reported,[18] we obtained an estimate of the apparent standard rate constant of $Fe(CN)_6^{4-}$ at the $C_{18}SH$/Au electrode, by simulation of the cyclic voltammograms by a model for an electrode reaction at a covered electrode with reaction only at pinholes. The mathematics for this situation follows the CEC mechanism (Scheme 1).[33] From the minimal values of the chemical reaction parameters ($K = 5 \times 10^{-5}$; $k_1 = 10^5$ s^{-1}; $k_2 = 2 \times 10^9$ s^{-1}), which can be related to surface coverage and pinhole radius, we could obtain an estimate of the surface coverage, $\theta \approx 0.999\,95$, and of the pore radius, $R_d \approx 1$ nm, as

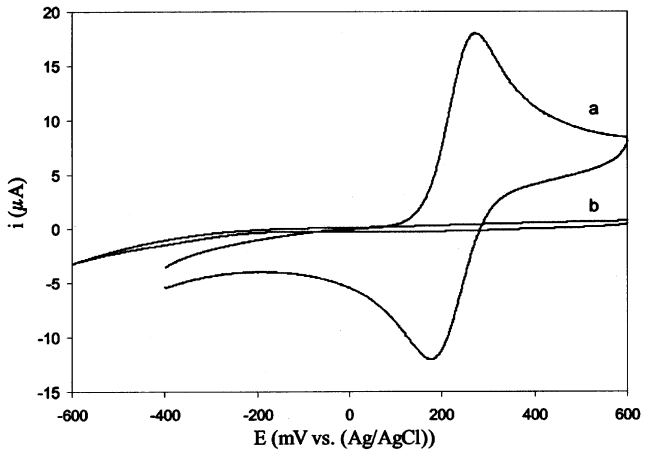

Figure 1. Cyclic voltammograms of a water solution containing $Na_4Fe(CN)_6$ (1 mM) in phosphate buffer (pH = 2.9; 0.2 M) at ν = 0.1 V s^{-1} on (a) a gold electrode (0.07 cm^2) and (b) an octadecanethiol monolayer adsorbed on a gold electrode.

Scheme 1

$$\mathrm{I} \underset{k_2}{\overset{k_1}{\rightleftharpoons}} \mathrm{A} \qquad \mathrm{C} \qquad (K = k_1/k_2)$$

$$\mathrm{A} + 1\,e \rightleftharpoons \mathrm{B} \qquad \mathrm{E} \qquad (E^0, \alpha, k^0)$$

$$\mathrm{B} \underset{k_1}{\overset{k_2}{\rightleftharpoons}} \mathrm{J} \qquad \mathrm{C} \qquad (1/K = k_2/k_1)$$

(21) Tsionsky, M.; Bard, A. J.; Mirkin, M. V. *J. Am. Chem. Soc.* **1997**, *119*, 10785.
(22) Tsionsky, M.; Zhou, J.; Amemiya, S.; Fan, F.-R. F.; Bard, A. J.; Dryfe, R. A. W. *Anal. Chem.* **1999**, *71*, 4300.
(23) Amemiya, S.; Ding, Z.; Zhou, J.; Bard, A. J. *J. Electroanal. Chem.* **2000**, *483*, 7.
(24) Amemiya, S.; Bard, A. J. *Anal. Chem.* **2000**, *72*, 4940.
(25) Slevin, C. J.; Ryley, S.; Walton, D. J.; Unwin, P. R. *Langmuir* **1998**, *14*, 5331.
(26) Yasukawa, T.; Uchida, I.; Matsue, T. *Biochim. Biophys. Acta* **1998**, *1369*, 152.
(27) Grimaldi, J. J.; Boileau, S.; Lehn, J. M. *Nature* **1977**, *265*, 229.
(28) Pierrat, O.; Lechat, N.; Bourdillon, C.; Laval, J.-M. *Langmuir* **1997**, *13*, 7085.
(29) Terrettaz, S.; Becka, A. M.; Traub, M. J.; Fettinger, J. C.; Miller, C. J. *J. Phys. Chem.* **1995**, *99*, 11216 and references therein.
(30) Marecek, V.; Samec, Z.; Weber, J. *J. Electroanal. Chem.* **1978**, *94*, 169.
(31) Slevin, C. J.; Ryley, S.; Walton, D. J.; Unwin, P. R. *Langmuir* **1988**, *4*, 5331.
(32) Porter, M. D.; Bright, T. B.; Allara, D. L.; Chidsey, C. E. D. *J. Am. Chem. Soc.* **1987**, *109*, 3559.
(33) Amatore, C.; Savéant, J.-M.; Tessier, D. *J. Electroanal. Chem.* **1983**, *147*, 39.

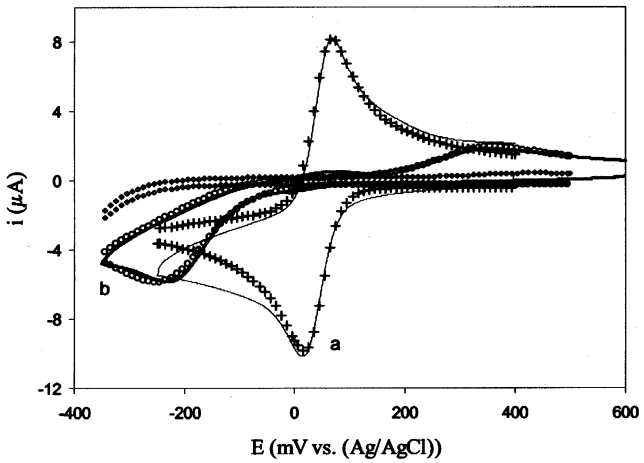

Figure 2. Cyclic voltammograms of menadione (0.2 mM) in phosphate buffer (pH = 2.9; 0.2 M) at $v = 0.1$ V s^{-1} at (a) a gold electrode (0.07 cm^2) and (b) an octadecanethiol monolayer adsorbed on a gold electrode. (+) curve simulated with a E_1E_2 mechanism with the following values: $E_1 = 0.025$ V; $\alpha_1 = 0.5$; $k_{s1} = 10^{-2}$ cm s^{-1}; $E_2 = 0.063$ V; $\alpha_2 = 0.5$; $k_{s2} = 10^{-1}$ cm s^{-1}. (◆) curve simulating the pore effect with a CE_1E_2C mechanism with the following chemical reaction parameters: $K = 5 \times 10^{-5}$; $k_{1c} = 10^5$ s^{-1}; $k_{2c} = 2 \times 10^9$ s^{-1}; $K' = 2 \times 10^4$; $k'_{1c} = 2 \times 10^9$ s^{-1}; $k'_{2c} = 10^5$ s^{-1}. (○) curve simulating permeability with a CE_1E_2C' mechanism with the following chemical reaction parameters: $K = 3.5 \times 10^{-3}$; $k_{1c} = 7 \times 10^3$ s^{-1}; $k_{2c} = 2 \times 10^6$ s^{-1}; $K' = 5 \times 10^3$; $k'_{1c} = 10^8$ s^{-1}; $k'_{2c} = 2 \times 10^4$ s^{-1}.

discussed in our previous work.[18] From the apparent electron transfer rate constant decrease ($k^\circ_{CV} = k^\circ(1 - \theta) = 1.5 \times 10^{-6}$ cm s^{-1}) we conclude that the monolayer was not *totally* free from pinholes and that the electron transfer for ferrocyanide corresponds to oxidation at pinholes or defect sites.

For the menadione, we first simulated the cyclic voltammogram at the bare gold electrode to estimate the electron-transfer parameters. Laviron[34] showed that this type of reaction could be described as two successive electron transfers E_1E_2 with apparent electron-transfer rate constants that reflect pure electron transfer and protonation or deprotonation steps. Using such an E_1E_2 mechanism, one could simulate the cyclic voltammogram at pH = 2.9 with the following parameters:

$$E_1^\circ = 0.025 \text{ V}; \quad \alpha = 0.5; \quad k_1^\circ = 10^{-2} \text{ cm s}^{-1} \quad (2)$$

$$E_2^\circ = 0.063 \text{ V}; \quad \alpha = 0.5; \quad k_2^\circ = 10^{-1} \text{ cm s}^{-1} \quad (3)$$

The system is quite complex and also involves proton transfers that we assume to be rapid. In fact, the curve could be simulated with other k_2° values, and so we have chosen arbitrarily to take the smallest one.

To compare the electrochemical behavior of the menadione and the $Fe(CN)_6^{4-}$, at the $C_{18}SH$/Au electrode, we first simulated the cyclic voltammogram of menadione assuming a pinhole model (i.e., a CE_1E_2C mechanism) while keeping the chemical reaction parameters obtained for $Fe(CN)_6^{4-}$ reduction at the covered electrode and the electron-transfer parameters obtained for the menadione without the monolayer. Under such conditions, the simulated curve is represented in Figure 2 (◆). So, if the menadione redox process occurs by diffusion through the pores such as for $Fe(CN)_6^{4-}$, the reduction would require

(34) Laviron, E. *J. Electroanal. Chem.* **1984**, *164*, 213.

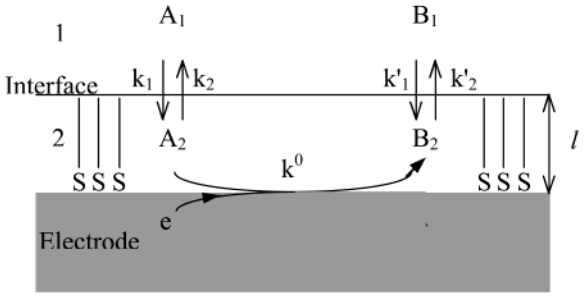

Figure 3. Schematic representation of the partitioning of reactants A and B between phases 1 and 2.

an overpotential larger than 400 mV. Figure 2b shows that when the monolayer is adsorbed on the gold electrode, we observe an experimental wave with a much smaller overpotential (i.e., anodic and cathodic peak potentials are spaced from those of curve a by only about 250 mV) with a simultaneous decrease of the peak currents. Since the overpotential is much less important than that for $Fe(CN)_6^{4-}$, the menadione redox process at the $C_{18}SH$/Au electrode is unlikely to proceed by diffusion through the pores, but rather occurs by permeation into the monolayer. This supposition is also supported by the reported trapping of menadione into a thiol monolayer covering a gold electrode.[11] In this reference, the possible partitioning between the monolayer and the aqueous phase was suggested by the partial loss of menadione after the tenth cyclic voltammogram.

Estimation of Permeability by Cyclic Voltammogram Simulation. A simple one-electron transfer coupled to possible partitioning of the reactants between two phases, when the electrode is in contact with one, as depicted in Figure 3 can be described by the following set of equations:

$$A_1 \underset{k_2}{\overset{k_1}{\rightleftarrows}} A_2 \quad K = k_1/k_2 \quad (4)$$

$$A_2 + e \rightleftarrows B_2 \quad E^\circ, k_0 \quad (5)$$

$$B_1 \underset{k'_2}{\overset{k'_1}{\rightleftarrows}} B_2 \quad K' = k'_1/k'_2 \quad (6)$$

where the partition equilibria (eqs 4 and 6) occur at the interface between 1 and 2. This situation can be described theoretically by the solution of the diffusion equation (eq 7) for reactants A and B in both phases ($i = 1, 2$):

$$\frac{\partial A_i}{\partial t} = D_i \frac{\partial^2 A_i}{\partial x^2} \quad (7)$$

according to the following boundary conditions pertinent to the problem:

$x = l$ (interface)

$$D_1 \left.\frac{\partial A_1}{\partial x}\right|_{x=l} = D_2 \left.\frac{\partial A_2}{\partial x}\right|_{x=l} = k_1 A_1|_{x=l} - k_2 A_2|_{x=l} \quad (8)$$

$$D_1 \left.\frac{\partial B_1}{\partial x}\right|_{x=l} = D_2 \left.\frac{\partial B_2}{\partial x}\right|_{x=l} = k'_1 B_1|_{x=l} - k'_2 B_2|_{x=l} \quad (9)$$

with $K = k_1/k_2$ and $K' = k'_1/k'_2$ pertaining to the heterogeneous equilibria (eqs 4 and 6).

$x = 0$ (electrode surface)

$i = nFSk_0$

$$(A_2|_{x=0} \exp(-\alpha F(E - E^\circ)/RT) - B_2|_{x=0} \exp((1 - \alpha)F(E - E^\circ)/RT)) = nFSD_2 \frac{\partial A_2}{\partial x}|_{x=0} = -nFSD_2 \frac{\partial B_2}{\partial x}|_{x=0} \quad (10)$$

These equations are more easily handled when recast in their dimensionless forms with the help of the following dimensionless constants

$$y = \frac{x}{\sqrt{D_2\tau}} \qquad \tau = RT/Fv$$

$$L = \frac{l}{\sqrt{D_2\tau}}, \quad \lambda_i = \frac{k_i}{\sqrt{D_1/\tau}}, \quad \Lambda = \frac{k_0}{\sqrt{D_1/\tau}}, \quad D^* = D_1/D_2$$

and the following dimensionless current and potential

$$\Psi = \frac{i}{nFS\sqrt{D_1/\tau}C^*}$$

where C^* is the initial total concentration of the species

$$\xi = -F/RT(E - E^\circ)$$

One can assume that in the small phase layer covering the electrode the concentration varies linearly with the distance x. Henceforth, the solution of this set of equations leads to the following expression of the dimensionless current:

$$\Psi = \Lambda \exp(\alpha\xi)\left[K\left(1 - \Psi\frac{(1 + D_1L/D_2)}{K\lambda_2} - I\Psi\right) - K' \exp(-\xi)\left(\Psi\frac{(1 + D_1L/D_2)}{K'\lambda'_2} + I\Psi\right)\right] \quad (11)$$

where $I\Psi$ is the convolution of the dimensionless current expressed by

$$I\Psi = \int_0^\tau \frac{\Psi(\eta)}{\sqrt{\pi(\tau - \eta)}}\,d\eta \quad (12)$$

One can show that this expression is identical to that for the current obtained for a CEC mechanism such as

$$Z \underset{k_{2c}}{\overset{k_{1c}}{\rightleftharpoons}} A \quad K_c = k_{1c}/k_{2c} \quad (13)$$

$$A + e \rightleftarrows B \quad E^\circ, k_0$$

$$B \underset{k'_{2c}}{\overset{k'_{1c}}{\rightleftharpoons}} C \quad K'_c = k'_{1c}/k'_{2c} \quad (14)$$

with

$$K = K_c/(1 + K_c) \quad (15a)$$

and

$$K_c\sqrt{\lambda_c} = \frac{K\lambda_2}{1 + D_1L/D_2} \quad (16a)$$

Scheme 2

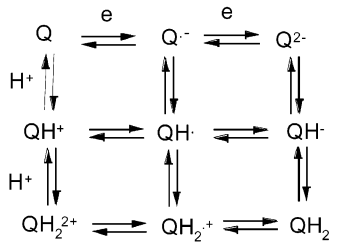

for the preequilibrium, and

$$K' = 1/(1 + K'_c) \quad (15b)$$

and

$$\frac{\sqrt{\lambda'_c}}{K'_c} = \frac{K'\lambda'_2}{1 + D_1L/D_2} \quad (16b)$$

for the postequilibrium, where the dimensionless homogeneous rate constants are given as $\lambda_c = (k_{1c} + k_{2c})RT/Fv$.

This simple model shows that the partitioning of the reactants between the aqueous phase and the monolayer can then be quantified by the CV experiment and can be simulated by a CEC′ mechanism. The values of the partition constants and heterogeneous rates (k_1, k_2, k'_1, and k'_2 in cm s^{-1}) can be obtained from the values of the corresponding simulated chemical equilibrium constants and homogeneous rates ($k_c = k_{1c} + k_{2c}$ and $k'_c = k'_{1c} + k'_{2c}$ in s^{-1}) from eqs 15 and 16 as

$$k_1 = K_c\sqrt{k_cD_1} \quad \text{and} \quad k_2 = (1 + K_c)\sqrt{k_cD_1} \quad (17)$$

$$k'_1 = \sqrt{k'_cD_1}/K'_c \quad \text{and} \quad k'_2 = (1 + K'_c)\sqrt{k'_cD_1}/K'_c \quad (18)$$

if one can neglect the diffusion limitation in the monolayer ($D_2/L \gg D_1$).

We have then attempted to apply this simple model to explain menadione reduction at the $C_{18}SH$/Au electrode. This approach, consisting of using the CE_1E_2C' model to simulate the CV response at the filmed electrode, is simple and rough, as the E_1 and E_2 steps were deduced from the simulation of the electrochemical response at a bare gold electrode. Indeed, the electrochemical parameters should not be exactly the same because the electron transfer does not occur in the same medium: water for the bare electrode and organic medium for the modified electrode, as the monolayer can be considered as a thin organic film. However, this approach is useful in obtaining a qualitative analysis of the menadione reduction at the $C_{18}SH$/Au electrode over the whole pH range investigated. As can be seen in Figure 2, the simulation fits the experimental curves quite well and is a reasonable first approximation.

Effect of pH on Menadione Reduction at Au and $C_{18}SH$/Au Electrodes. The general mechanism of quinone electrochemical behavior, represented in Scheme 2, can be decomposed into four elementary steps involving sequential transfer of either one electron or one proton. Thus, there are six different mechanisms involving nine different possible quinone species that are described in this square scheme.[5,34]

As menadione reduction involves the transfer of two protons, we have analyzed the effect of the pH on the cyclic voltammogram at the monolayer modified gold electrode. Figures 2 and 4 show that the cathodic peak potential shifts to more negative values (by about 60 mV per pH unit). While the anodic peak potential decreases

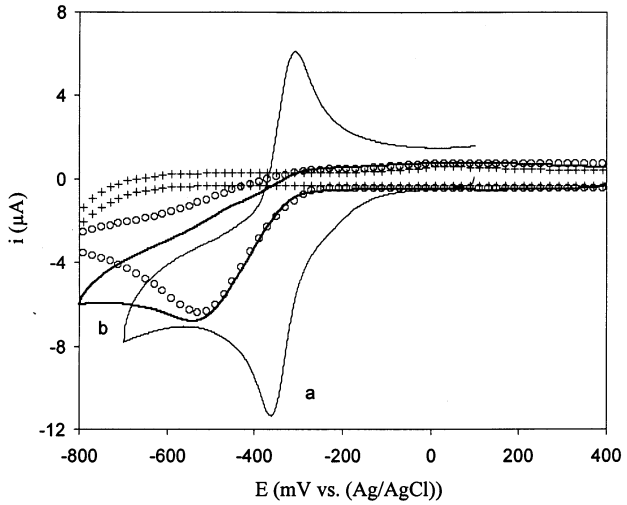

Figure 4. Cyclic voltammograms of menadione (0.2 mM) in phosphate buffer (pH = 9.3; 0.2 M) at $v = 0.1$ V s^{-1} at (a) a gold electrode (0.07 cm^2) and (b) an octadecanethiol monolayer adsorbed on gold electrode. (+) curve simulating the pore effect with a CE_1E_2C mechanism with the following chemical reaction parameters: $E_1 = -0.352$ V; $\alpha_1 = 0.4$; $k_{s1} = 1.5 \times 10^{-2}$ cm s^{-1}; $E_2 = -0.312$ V; $\alpha_2 = 0.5$; $k_{s2} = 10^{-1}$ cm s^{-1}; $K = 5 \times 10^{-5}$; $k_{1c} = 10^5$ s^{-1}; $k_{2c} = 2 \times 10^9$ s^{-1}. (○) curve simulating the permeability with a CE_1E_2C' mechanism with the same electron transfers parameters and $K = 3 \times 10^{-2}$; $k_{1c} = 10^6$ s^{-1}; $k_{2c} = 3.3 \times 10^7$ s^{-1}; $K' = 8 \times 10^4$; $k'_{1c} = 3 \times 10^7$ s^{-1}; $k'_{2c} = 3.8 \times 10^2$ s^{-1}.

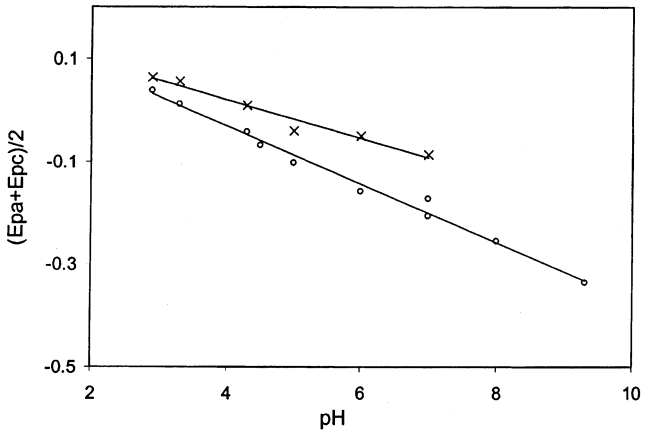

Figure 5. Variation of the half sum of the anodic and cathodic peak potentials, for the menadione/menadiol redox couple (○) at the gold electrode and (×) at the $C_{18}SH$/Au electrode.

by about 20 mV per pH unit, its intensity decreases drastically when the pH increases, so that the reoxidation is almost absent at pH 9.3. Figure 5 shows the variation of the average of the anodic and cathodic peak potentials for the reduction of menadione with pH at the bare and at the monolayer modified gold electrodes. This average can be considered approximately as the standard (formal) potential. At the bare gold electrode, the standard potential (and the cathodic and anodic peak potentials) decreased by about 60 mV per pH unit, corresponding to a two-electron−two-proton overall redox process. On the other hand, at the monolayer modified gold electrode, although the cathodic peak potential still decreased by 60 mV per pH unit, the anodic peak potential, when it could be detected, decreased by less than 20 mV per pH unit. The variation of the cathodic peak potential with pH tends to indicate that, whether covered by a monolayer or not, the protonation sequences involved during or before the rate-limiting step of the reduction are unchanged. The permeation does not affect the chemistry of the reduction stage. On the other hand, the smaller variation of the anodic branch and the decrease of the anodic peak current with pH are consistent with a pH-dependent loss of the reduced species formed upon reduction of menadione. This significant loss intervenes in the rate-limiting step of the oxidation stage, explaining the change in the pH effect. It leads to a decrease in the apparent standard reduction potential, where it can be defined, by only 35 mV per pH unit, approaching the value obtained for an overall two-electron−one-proton redox process.

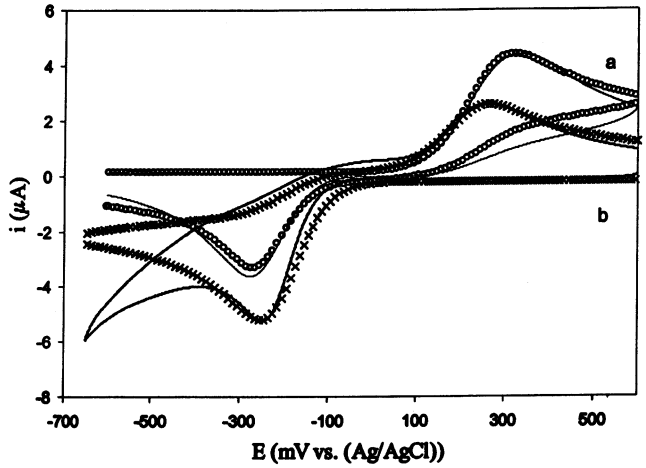

Figure 6. Cyclic voltammogram (a) of menadiol (0.27 mM) and (b) of menadione (0.2 mM) in phosphate buffer (pH = 4; 0.2 M) at $v = 0.1$ V s^{-1} at an octadecanethiol monolayer adsorbed on a gold electrode (0.07 cm^2). (○ and ×) curves simulating permeability with a CE_1E_2C' mechanism with the following parameters: $E_1 = -0.056$ V; $\alpha_1 = 0.4$ (○) and 0.6 (×); $k_{s1} = 1.5 \times 10^{-2}$ cm s^{-1}; $E_2 = -0.024$ V; $\alpha_2 = 0.5$; $k_{s2} = 10^{-1}$ cm s^{-1}; $K = 10^{-4}$ (○) and 6×10^{-3} (×); $k_{1c} = 2 \times 10^4$ s^{-1} (○) and 1.5×10^3 s^{-1} (×); $k_{2c} = 2 \times 10^8$ s^{-1} (○) and 2.5×10^5 s^{-1} (×); $K' = 3 \times 10^2$ (○) and 4.1×10^3 (×); $k'_{1c} = 2 \times 10^8$ s^{-1} (○) and 8×10^7 s^{-1} (×); $k'_{2c} = 6.7 \times 10^5$ s^{-1} (○) and 2×10^4 s^{-1} (×).

This loss is clearly related to the presence of the monolayer, since this effect is not observed at the bare gold electrode and since it is also observed at the level of the menadiol oxidation at a $C_{18}SH$/Au electrode. Indeed, as can be seen in Figure 6, menadiol oxidation at pH 4 leads to a reversible oxidation−reduction, but with peak currents lower than those observed for the menadione reduction.

We can propose two different explanations for the pH-dependent loss of the menadiol or of the reduced intermediates of menadione at $C_{18}SH$/Au electrodes. The first is based on permeation only and supposes the involvement of reduced species whose partition toward the aqueous phase is enhanced when the pH is increased. In terms of the permeation model indicated earlier, in chemical terms, this means that the equilibrium constant in C′ is higher than that in C. The second implies a true chemical instability in the monolayer of one of the intermediate species formed upon the reduction of the menadione in the presence of water. This hypothesis is in agreement with the analysis of Cauquis and Marbach of the electrochemical behavior of quinones in organic solvents in the presence of water.[37]

Cauquis and Marbach[35] proposed two mechanisms for the oxidation of menadiol in an organic solvent as a function of pH. Scheme 3 corresponds to the mechanism in an organic medium in the presence of water and in an

(35) Cauquis, G.; Marbach, G. *Bull. Soc. Chim. Fr.* **1971**, *5*, 1908.

Scheme 3

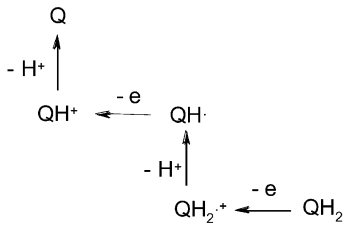

Scheme 4

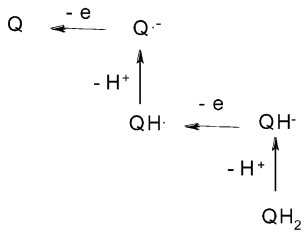

acidic medium where the first step is oxidation to the cation radical. Scheme 4 corresponds to the mechanism in basic medium, with an initial deprotonation step. If one considers the permeation of species into the monolayer, the electron transfer does not occur in the same medium when the electrode is gold or gold modified by a monolayer. Indeed, as we mentioned above, the monolayer can be considered as a thin organic film. So, as the menadione and menadiol permeate the monolayer, the redox process at the $C_{18}SH$/Au electrode occurs in an organic solvent in the presence of water rather than in water, as at the bare Au electrode. Thus, the menadiol oxidation mechanism inside the monolayer is closer to that in an organic solvent as described by Schemes 3 and 4. Since the intermediates involved are different as the pH is changed, the species involved at basic pH are perhaps less stable in the monolayer than the species involved at acidic and neutral pH values. Therefore, at basic pH, the species could react differently and permeate more slowly, because they are more hydrophilic than the species involved in acidic and neutral media. In any event, these two different phenomena will tend to lower the apparent permeability of the menadiol or the reduced menadione species at basic pH, as observed by CV.

To a first approximation, we interpret this loss of reversibility by a change in partitioning of the reduced species. In this manner, we could use the model indicated earlier to simulate the cyclic voltammograms observed for the menadione reduction or the menadiol oxidation at different pH values. The menadione behavior was examined between pH 2.9 and pH 9.3. The menadiol behavior was examined only at pH 4 and 7 because of its relative instability at basic pH, as mentioned by Cauquis and collaborators.[35] For that purpose we have adopted the strategy used to simulate the pH 2.9 voltammograms. For any given pH, we started by simulating the bare Au electrode behavior (not available for the menadiol) by an E_1E_2 mechanism and using these parameters in the more complex CE_1E_2C' mechanism for the simulation of the permeation process at the $C_{18}SH$/Au electrode. Some examples of this simulation are shown, along with the experimental curves, in Figures 2, 4, and 6. They show that the fit is quite good. Moreover, the menadiol oxidation should present a situation symmetrical to the menadione reduction. Thus, the parameters used to simulate the menadione reduction by the permeation mechanism CE_1E_2C' were reversed into a $C''E_2E_1C'''$ mechanism. This implies that the parameters for the C″ and C‴ steps are

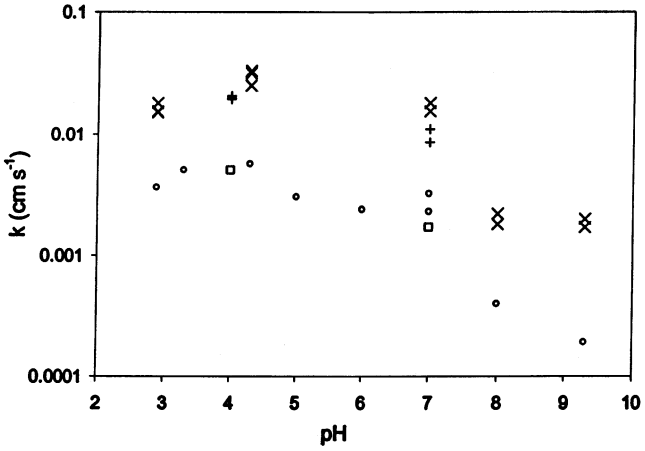

Figure 7. Variation of the permeability with pH estimated by cyclic voltammetry (□ and ○) and by SECM (+ and ×) for a phosphate buffer solution containing 0.2 mM menadione (○ and +) or 0.27 mM menadiol (□ and ×).

easily obtained, since they are respectively reverse reactions of C′ and C. The simulation was started with these parameters, and a best fit of the menadiol behavior at pH 4 was obtained for parameters close to the chosen ones (Figure 6). Considering that a new and fresh monolayer was deposited before each different trial, the agreement of simulation and experiment can be considered satisfactory.

We then extracted from the simulated menadione and menadiol cyclic voltammograms and from eqs 17 and 18 an apparent rate-limiting permeability coefficient for the different pH values studied (Figure 7) as the minimum value of the heterogeneous rate constants corresponding to the pre- and postequilibrium (eqs 4 and 5), respectively:

$$k_{CV,perm} = 1/(1/k_1 + 1/k_2 + 1/k'_1 + 1/k'_2) \approx \min(k_1, k_2, k_1', k_2') \quad (19)$$

First, note that the values obtained for menadiol oxidation are close to those for the menadione reduction at the same pH. This is consistent with the fact that the permeation through the monolayer on the gold electrode is limited by the smallest partition rate, apparently that of the reduced species. Second, Figure 7 shows that the permeability is constant until pH 7 and then decreases at basic pH. This result can be related to the loss of the anodic peak observed on the reverse scan for the cyclic voltammogram at basic pH and explained by the loss from the monolayer of one of the reduced species of the menadione at this pH. Because of the complexity of the system, we have, in a first approximation, considered that mass transfer through pinholes or defect sites can be neglected. As discussed later, this is certainly true for pH < 7, but this phenomenon could be more important at higher pH. As we do not know precisely the pore contribution for each monolayer studied, we did not take it into account. However, if we assume that we are able to obtain reproducible coverage (attested by the reproducibility of the voltammograms or SECM approach curves from one experiment to another), we could estimate the portion of the pore contribution in the voltammetric response at alkaline pH. We then simulated the cyclic voltammogram of menadione assuming a pore model (i.e., a CE_1E_2C mechanism, as explained for Figure 2) while keeping the chemical reaction parameters obtained for $Fe(CN)_6^{4-}$ reduction at the covered electrode and the electron transfer

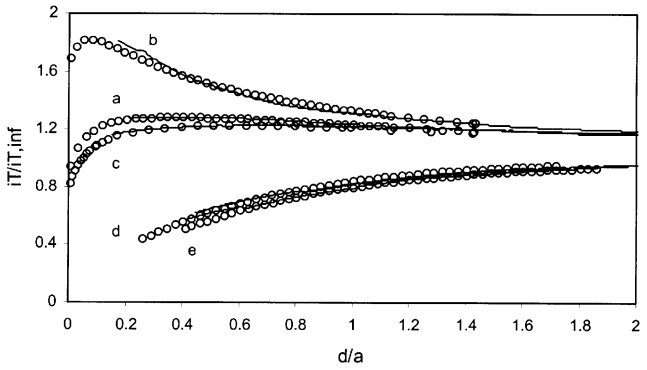

Figure 8. Current−distance curves for a 3.5-μm-radius C tip UME approaching a gold substrate covered by an octadecanethiol monolayer in an aqueous solution containing 0.2 mM menadione in phosphate buffer (0.2 M) at pH = (a) 2.9; (b) 4.3; (c) 7; (d) 8; and (e) 9.3. The tip was biased at −0.4 V (a); −0.45 V (b); −0.55 V (c); −0.65 V (d); and −0.7 V (e). The substrate was biased at 0.6 V (a−c); 0.4 V (d); and 0.3 V (e). The tip scan rate was 1 μm s^{-1}. The solid lines correspond to the experimental curves, and the dashed lines, to SECM theory (eq 20) with apparent heterogeneous rate constant k_{SECM} = 0.018 cm s^{-1} (a); 0.033 cm s^{-1} (b); 0.018 cm s^{-1} (c); 0.0018 cm s^{-1} (d); and 0.002 cm s^{-1} (e).

parameters obtained for the menadione without the monolayer. Under such conditions, we could observe that the simulated reoxidation wave was always lower than the experimental one. However, at pH 9.3 (Figure 4), the simulated reoxidation wave was almost as high as the experimental one, indicating that, at this pH, diffusion through pores is certainly the major contribution to the reoxidation process and that the estimated permeation rate constant at this pH should be even lower than the value proposed earlier. It is unreasonable to go into a more detailed analysis that would take into account both pore and permeation effects, and we adopted the value obtained from the permeation model, keeping in mind that this apparent value is overestimated.

Estimation of the Permeability through the Monolayer by SECM. As the cyclic voltammogram simulation allows only a qualitative analysis, we have also used the scanning electrochemical microscope to evaluate more quantitatively the permeability of the menadione through the monolayer adsorbed on the gold electrode. The approach curves were taken at different pH values with a carbon UME tip (radius, a = 3.5 mm) approaching a C_{18}SH/Au substrate in a solution containing menadione in phosphate buffer (Figure 8). The potentials applied at the tip and gold substrate were chosen from cyclic voltammograms so as to generate the menadiol in water at the tip and to oxidize it back to menadione at the substrate under diffusion-controlled conditions. Although the electron-transfer kinetics at the tip and Au substrate are rapid, the approach curves show kinetic limitations. The analytical treatment that describes finite heterogeneous kinetics at the substrate can be used to describe the overall process. The expression of the tip current is given as a function of the normalized tip−substrate separation ($L = d/a$) as[15,16]

$$I_T^K = \left[\frac{0.78377}{L(1 + 1/\Lambda)} + \frac{0.68 + 0.3315\exp(-1.0672/L)}{1 + F(L,\Lambda)}\right] \times (1 - I_T^{ins}/I_T^c) + I_T^{ins} \quad (20)$$

where I_T^c and I_T^{ins} represent the tip current for the conductive and insulating substrates, respectively. The expressions for these as a function of the normalized distance $L = d/a$ are

$$I_T^c = 0.78377/L + 0.3315\exp(-1.0672/L) + 0.68 \quad (21)$$

$$I_T^{ins} = 1/(0.15 + 1.5358/L + 0.58\exp(-1.14/L) + 0.0908\exp[(L - 6.3)/(1.017L)] \quad (22)$$

where $\Lambda = kd/D$, with k the apparent limiting heterogeneous rate constant, D the aqueous diffusion coefficient ($D = 5.5 \times 10^{-6}$ cm^2 s^{-1}), and $F(L,\Lambda) = [(11 + 7.3\Lambda)/\Lambda]/(110 - 40L)$.

I_T^K, I_T^c, and I_T^{ins} are normalized by the tip current at an infinite tip−substrate distance ($i_{T,\infty} = 4nFaDC$°).

Under these SECM conditions, the redox process at the modified electrodes should be limited by mass transport through the monolayer rather than by the electron transfer.[17,18,36] The apparent limiting heterogeneous rate constant obtained by simulation of the approach curves should then correspond to the rate-limiting mass transport. We have simulated the approach curves obtained for menadione (Figure 8) regeneration at the C_{18}SH/Au electrode at different pH values by using the theoretical expression, eq 20. The apparent limiting heterogeneous rate constants obtained by SECM are reported in Figure 7. We have also gathered in this figure the results for menadiol regeneration, obtained from the treatment of the curves corresponding to the approach of a carbon UME tip toward a C_{18}SH/Au electrode in a solution containing menadiol in phosphate buffer at pH 4 and 7. In this case, the tip potential was chosen so as to generate the menadione in water and the substrate potential was biased so as to reduce it back to menadione. The rate constants for the menadiol regeneration obtained at pH 4 and 7 are close to those obtained for the menadione one. This tends to confirm that, under SECM conditions, the redox process at the modified electrode is limited by the slowest mass transport through the monolayer and that this limiting step should probably be the same for menadione reduction and menadiol oxidation at the C_{18}SH/Au electrode. This situation is actually similar to the conclusion drawn from the cyclic voltammetric experiments. We then believe that the apparent rate constant determined by SECM corresponds to the permeability through the monolayer of the species involved in the redox processes (one of the quinone species or proton). Moreover, the values we have obtained at neutral pH are similar to the permeation rate constant of 2 × 10^{-2} cm s^{-1} measured for the permeation of hydroquinone through a protoplast membrane.[26]

Figure 7 also shows that the results obtained by SECM are in good agreement with those obtained by CV, since we observe the same trends for the variation of the permeability with the pH. Indeed, the apparent rate constant k_{SECM} is quite constant until pH 7 and decreases for pH values higher than 7. This can clearly be related to the decrease in the anodic peak current at pH 8 and 9.3 and can be attributed, as discussed earlier, to a smaller permeability of a quinonoid species or of a proton into the monolayer or to a chemical instability of a reduced quinonoid species in the monolayer. From this hypothesis, menadione regeneration should be slower at basic pH than in acidic or neutral media.

In addition to the menadione regeneration occurring by permeation−reduction, the regeneration of this species can also take place by diffusion through pores in the film

(36) Marcus, R. A. *J. Chem. Phys.* **1956**, *24*, 4966.

and reduction. Since these processes occur at different sites on the electrode, the apparent rate constant k_{SECM} can then be roughly considered as the addition of both processes, permeation and diffusion through the pores:

$$k_{SECM} = k_{SECM,pores} + k_{SECM,permeability} \quad (23)$$

At pH 8 and 9.3, the apparent rate constant, k_{SECM}, corresponds to the sum of a low permeability and diffusion through the pores. An estimate of the pore contribution can be obtained from the values of the pore radius and surface coverage as[17]

$$k_{SECM,pores} = \frac{4(1-\theta)D}{\pi R_d} \quad (24)$$

As a rough estimate, $k_{SECM,pores} \approx 0.004$ cm s^{-1}, obtained from the simulation of the CV of the ferrocyanide reduction at the gold covered electrode, is in agreement with the experimental value of 0.002 cm s^{-1} measured at pH values higher than 7 by SECM.

Finally, although we could observe in Figure 7 the same trends in the variation of the permeability estimated by CV and by SECM with pH, the values obtained by SECM are 2 times higher than those obtained by CV. The analysis applied to simulate the approach curves requires fewer parameters and should only depend on the mass transport processes. The time-dependent situation observed at the level of the CV is certainly richer in information, but it is thus more complex. Indeed, because the menadione redox process involves electron and proton transfers, it is quite difficult to simulate the behavior accurately, as it involves many more parameters. For example, for the sake of simplicity of the simulation of the cyclic voltammogram at the $C_{18}SH$/Au electrode, we have arbitrarily taken the electron transfer at the gold covered electrode to be described by the same parameters as those obtained at the bare gold electrode. This should not be true, as the electron transfer does not occur in the same medium (water at the bare gold electrode and organic medium at the $C_{18}SH$/Au electrode). Moreover, there is a possible tunneling effect at the $C_{18}SH$/Au and the reactivity of the possible intermediates (and thus the reduction mechanism) should differ. Because of the satisfactory agreement of the simpler CV simulation and because of the complexity of the more detailed case, we did not attempt a deeper analysis of the CV.

Conclusion

In conclusion, we have confirmed that the self-assembly method allows the easy preparation of a stable monolayer supported on gold. The surface coverage, calculated by cyclic voltammetric simulation, is 0.999 95. This coverage is high enough to induce a high decrease in the apparent standard rate constant for ferrocyanide oxidation. Because the monolayer acts as an electron and ion barrier for this hydrophilic compound, the reaction occurs by diffusion through pinholes and electron transfer at free sites on the electrode. Since menadione and menadiol are more hydrophobic, they can permeate the monolayer, and in this case, the redox process can occur at the electrode surface and the apparent standard rate constant does not decrease as much as that for $Fe(CN)_6^{4-}$, compared to the case of a bare gold electrode. The permeability of the menadione/menadiol couple through the monolayer can be evaluated by CV simulation using a simple model based on a CE_1E_2C' mechanism. However, this redox couple involves the transfer of two electrons and two protons and is quite complex. Thus, the simulation requires the estimation of a number of parameters, so the results are less precise and lead to a qualitative analysis. However, as in previous studies, SECM was shown to be a powerful technique to probe permeability through a monolayer. This was estimated by simulating the approach curve of an SECM tip to the monolayer adsorbed on the gold electrode. This treatment is more precise and easier than the analysis applied to determine the permeability by CV. However, despite the crudeness of the CV simulation, the trends observed by both techniques are alike. Furthermore, this technique was useful in elucidating the mechanism of the menadione redox process at a gold electrode modified by a monolayer. It suggests loss of a reduced species formed upon reduction of the menadione in the monolayer. This loss could be related to better affinity of this species for the aqueous phase (i.e. its rapid extraction out of the monolayer) or to its chemical decomposition in the monolayer. This work provides a better understanding of menadione behavior at a thiol monolayer, a biomimetic system, and our work is now focused on the behavior of this compound in real biological membranes and systems such as yeast cells.

Acknowledgment. This work has been supported by grants from the National Science Foundation (CHE-9870762) and the Robert A. Welch Foundation.

LA0258906